Characterisation and standardisation of different-origin end-of-life building materials for assessment of circularity

Emircan Ozcelikci[1,2,*],Gurkan Yildirim[2,3], Hocine Siad[4], Mohamed Lachemi[4], Mustafa Sahmaran[2]

[1] Institute of Science, Hacettepe University, Beytepe, Ankara, Turkey
[2] Department of Civil Engineering, Hacettepe University, Ankara, Turkey
[3] Department of Civil and Structural Engineering, University of Bradford, Bradford, the UK
[4] Department of Civil Engineering, Ryerson University, Toronto ON, M5B 2M2, Canada
[*] Corresponding author: e-mail: eozcelikci@hacettepe.edu.tr; emirozcelikci@gmail.com

Abstract

Construction and demolition waste (CDW) management and recycling practices are crucial for transitioning to a circular economy. This study focuses on the detailed characterization of CDWs, including hollow brick (HB), red clay brick (RCB), roof tile (RT), concrete (C), and glass (G), collected from seven different sites. The CDWs were characterized based on particle size distribution, chemical composition, and crystalline nature. Pozzolanic activity was evaluated through compressive strength measurements of cement mortars with 20% cement replacement by CDWs at 7, 28, and 90 days. The results showed that clayey CDWs exhibited similar physical/chemical properties and crystalline structures. Compositions of Cs varied significantly based on their original materials. CDWs satisfied the minimum strength activity index for supplementary cementitious materials, with pozzolanic activity influenced by fineness and SiO2+Al2O3 contents. The average strength activity indexes for HB, RCB, RT, C, and G were 84.5%, 86.3%, 83.4%, 80.7%, and 75.8%, respectively. Clayey CDWs contributed to mechanical strength development, while Cs' contribution was related to hydration of unreacted cementitious particles. G exhibited the weakest pozzolanic activity due to its coarser particle size. Overall, CDWs demonstrated suitable properties for use as supplementary cementitious materials in PC-based systems.

Keywords: Construction and demolition waste (CDW); Characterization; Physical and chemical properties; Circular economy; Pozzolanic activity; UN SDG 11 and 13.

1. Introduction

In today's world, in addition to the designs that make human life easier, the development of eco-friendly materials is of great importance. Every step that needs to be taken regarding the environmental, socio-economic and sustainability aspects is therefore critical to avert the issues like rapid consumption of natural resources, greenhouse gas emissions, and global warming.

Within this context, one of the leading materials to consider is concrete, which is the second most used material in the world after water (Scrivener and Kirkpatrick, 2008). Within the composition of traditional concrete, Portland cement (PC), which acts as the main binder for the material, is critically important, since its production requires high energy and raw materials consumption creating huge amounts of carbon emissions. For instance, a ton of manufactured PC clinker requires 850 kcal of energy and 1.7 tons of natural resources and is responsible for 0.94 tons of CO_2 release (Rashad and Zeedan, 2011; Praneeth et al., 2020). PC production is accountable for 5-8% of the total anthropogenic CO_2 in the atmosphere (Turner and Collins, 2013; Chan et al., 2015; Bakhtyar et al., 2017). Despite its drawbacks, the place of traditional concrete, and relatedly PC production, did not change over the years and the material is still the most commonly used construction material in the world (Stafford et al., 2016). Considering the increased number of activities related to the construction and demolition sector along with the requirements for the repetitive repair/retrofit/rehabilitation activities creating additional waste and necessitating more and more PC-based concrete-like materials, the development of more eco-friendly and sustainable alternative materials is necessary (Monteiro et al., 2017).

As abovenoted, the construction and demolition sector and activities related to it are booming in recent years. This can be mainly related to the continuously growing urban population and developing industries/economies of countries around the globe. Despite its commonness, the construction and demolition sector is one of the biggest contributors to solid waste production globally (Eurostat, 2015). The sector leads to different waste streams, which can be collectively termed as, “Construction and Demolition Waste (CDW)”. It has been reported that over 10 billion tons of CDW are generated worldwide each year (Wu et al., 2019), of which about 700 million tons are produced by the United States (Jain et al., 2015), 800 million tons by Europe (Ajayi et al., 2016) and 2.3 billion tons by China (Zheng et al., 2017). These wastes, which are likely to incorporate toxic substances, are usually dumped in clean landfills, thus jeopardizing the health of individuals and contaminating the surrounding environment (Roussat et al., 2008). Although the recycling of CDW has attracted the attention of the whole world in recent years, it is nevertheless estimated that more than 35% of CDWs are routinely diverted directly to clean landfills without any further process (Menegaki and Damigos, 2018). Therefore, it is crucial to handle CDW in an appropriate manner for the sake of environmental, social, and economic benefits. This is important both for reducing the quantities of CDW going to clean landfills and the amount of concrete material that is, otherwise, going to be used to build/repair/maintain new and/or existing infrastructures.

In order to tackle the CDW problem, transforming CDW-based materials into sustainable construction materials has attracted the growing attention of researchers. One of the recently trending ways to utilize CDWs is producing alkali-activated materials/geopolymers (Yildirim et al., 2021,2022; Ilcan et al., 2023; Mir et al., 2023; Ozcelikci et al., 2023a). A geopolymer is a binder obtained by the alkaline activation of solid alumina- and silica-containing precursors (Zhang et al., 2014). Considering that the most of CDW-based components are rich in alumina and silica, components derived from CDW can preferably be used in geopolymerization. As another trending method to recycle CDWs, partial replacement of CDWs with the clinker and/or PC is considered. A study replaced clinker with waste brick at various rates (0-20%) and found that higher waste brick content reduced setting times and grinding requirements (Naceri and Hamina, 2009). While the mechanical properties decreased after 7 and 28 days, they improved after 90 days, particularly with a 10% brick replacement ratio. In a study by Li et al. (2019), the effects of adding clay brick waste to mortars were evaluated. The compressive strength increased when cement paste was replaced by the waste, while the opposite trend was observed with cement powder replacement. The authors concluded that replacing paste with clay brick waste maintained a constant water/cement ratio, benefiting from the filler effect and promoting cement hydration. However, replacing cement powder led to a higher effective water/cement ratio, resulting in a negative effect.

Research conducted worldwide on the use of CDWs in cement-based and geopolymer systems has revealed variations in the performance of the final products, even when the mixture designs and curing processes are kept consistent. Notably, studies involving red clay brick activation using 10% Na_2O and thermal curing at around 70°C for 24 hours resulted in compressive strengths of approximately 10 MPa (Robayo-Salazar et al., 2017) and 6 MPa (Ulugöl et al., 2021) for geopolymers, respectively. These discrepancies can be attributed to the differences in the chemical composition of the red clay bricks obtained from different regions, despite similar volume mean diameters (both under 25 μm). Similarly, studies on brick waste-based geopolymer pastes using sodium hydroxide and sodium silicate as alkaline activators demonstrated compressive strengths of around 25 MPa (Komnitsas et al., 2015) and 38 MPa (Mahmoodi et al., 2020) under similar curing conditions. Differences were also observed in studies where CDWs were used as partial replacements in cement-based systems. For instance, the compressive strength of a mixture with a 15% replacement ratio outperformed a control sample (Oliveira et al., 2020), while another study reported that mixtures with replacement ratios of 20% and 30% exceeded the control mixture, reaching a maximum

compressive strength of 53 MPa after 28 days (Mucsi et al., 2021). The optimum replacement rate of CDWs is highly dependent on their origin and properties, underscoring the need for standardized characterization and technological guidelines (Cheng, 2016).

Considering the fact that construction and demolition is one of the five priority sectors designated by the European Action Plan, the necessary steps to shift CDWs from the "make-use-dispose" linear economy model to the circular economy model must be taken properly. In order to the integration of CDW into the circular economy, it must go through stages such as being properly managed, identified and ultimately included in the value chain by demonstrating the mechanical, economical, and environmental advantages of recycling/upcycling activities (Zhang et al., 2022; Ozcelikci et al., 2023b). Therefore, as the major target of this study, the characterization of different-origin CDWs for their further identification can be clearly considered one of the most important steps. The significance of this research lies in examining and uncovering the underlying mechanisms behind the variations in mechanical performance observed by researchers worldwide, despite similar formulations. By comprehensively investigating the effects of CDWs with different origins on the characteristics of the final product, this study aims to shed light on the factors influencing these variations. This, in turn, paves the way for optimizing CDW recycling practices by gaining a better understanding of the material and achieving maximum performance efficiency. In this study, hollow brick, red clay brick, roof tile, concrete and glass wastes from seven different demolition sites were considered under the same preparation and testing conditions. Particle size distribution, chemical composition and crystalline nature of each sample of CDW materials were thoroughly analyzed and compared to its strength activity indexes at 7, 28 and 90 days to determine their effectiveness as cementitious constituents. Microstructural analyses such as Scanning electron microscopy and Energy-dispersive X-ray spectroscopy (SEM/EDX) were conducted on the selected mixtures to validate and correlate obtained results. Additionally, the Thermogravimetry (TG/DTG) analysis was carried out to examine the reactivity and thermal behavior of CDW substitution in the PC system. The results obtained from this analysis provide valuable insights into the changes in reactivity, hydration characteristics, and thermal decomposition patterns, enabling a better understanding of CDW's performance as a PC substitute. The results are expected to provide an important database for industrials and researchers interested in the mass recycling of CDW materials, especially with the confusion and disagreement caused by the inconsistent results in the literature.

2. Experimental Program

2.1. Materials

CDW-based materials, including hollow brick (HB), red clay brick (RCB), roof tile (RT), concrete (C) and glass (G), were collected from seven urban transformation sites in Turkey after selective demolition. Fig. 1 shows a typical site with different CDW-based materials such as HB, RCB, RT, C and G. The same crushing/grinding procedures were applied for all raw CDWs. No special measures were taken to bring the waste materials to the same particle size distribution. As can be expected, in most demolition sites, the waste materials are present together and it is much less labor- and energy-intensive to recycle them without a specific preparation method. They were first subjected to initial crushing in a jaw crusher and reduced in size. Each CDW-based material was then loaded into a ball mill and grinded for an hour. Since the study deals with the characterization of different CDWs, the physical, chemical and mechanical properties of the wastes were presented in the following sections.

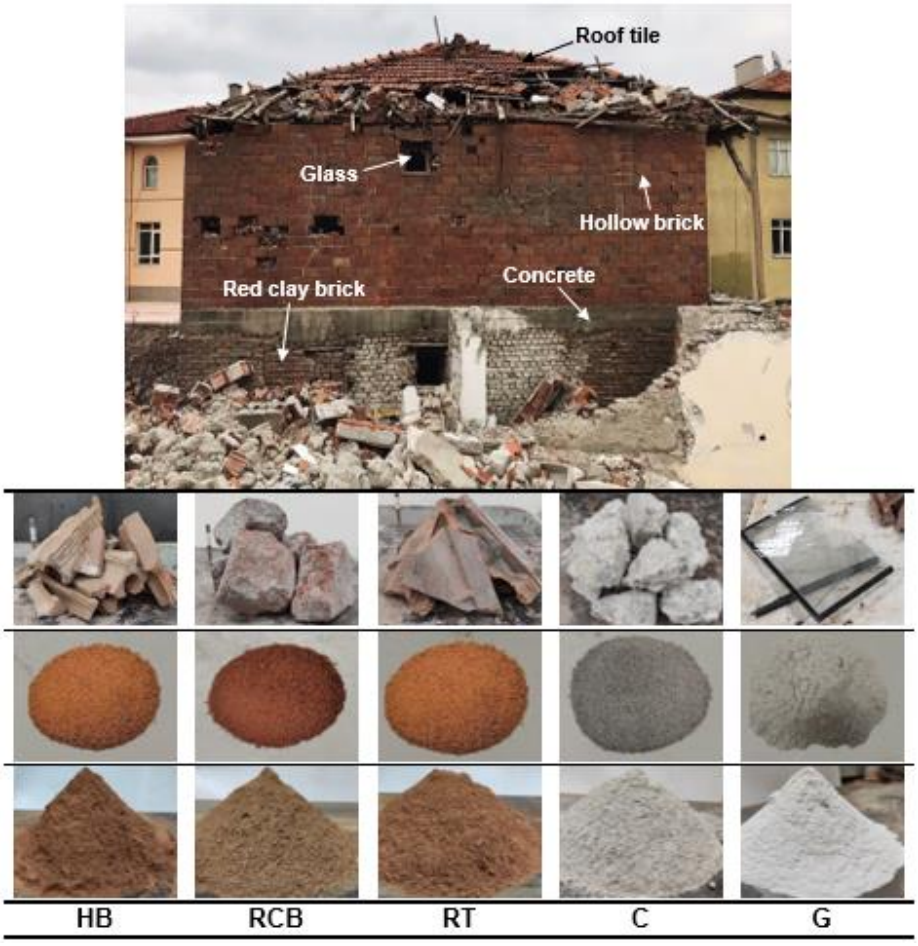

Fig. 1 A typical demolition site in Turkey and representative images of CDW-based materials before crushing, after crushing and after grinding

2.2. Methods

Analyses and tests for the determination of chemical composition, particle size distribution, crystalline structure and pozzolanic activity of powdery CDWs were performed. X-ray fluorescence (XRF) analysis was utilized to determine the chemical composition of the materials. Particle size distributions were determined by using dry laser granulometry method (Malvern Mastersizer Scirocco 2000 assembled with a hopper instrument). X-ray diffraction (XRD) analysis was performed to observe the crystalline nature of the materials, in which parameters such as scan range of $5° \leq 2\theta \leq 55°$, 2θ step length of 0.033°, a scanning step time of 30.48 s, and a wavelength Kα1 of copper (λ=1.5406Å) were used. Mortar specimens were produced in accordance with the ASTM C618-19 standard to measure the pozzolanic activity of materials (ASTM C618, 2019). The test was carried out on a control mixture proportioned with 500 g of Portland cement, 1375 g of sand and 242 g of water. Then, at the same amount of water usage as the control mixture, CDW-based compositions were designed by substituting 20% of PC with HB, RCB, RT, C or G. Compressive strength measurements were performed after 7, 28 and, 90 days by using three separate 50-mm cubic specimens for each age, in accordance with the ASTM C39-2021 standard (ASTM C39/39M, 2021). A loading device with 100-ton capacity and a loading rate of 0.9 kN/s was used for these tests. The strength activity index (SAI – %) was calculated as the ratio between the compressive strength of the CDW-substituted mortars and the control mixture. For in-depth microstructural characterization of selected mixtures, Scanning electron microscopy and Energy-dispersive X-ray spectroscopy (SEM/EDX) and Thermogravimetry (TG/DTG) were conducted. Specimens with dimensions less than 1 cm were used for the SEM/EDX analysis. To ascertain the temperatures at which the materials degraded, TG/DTG analyzes were carried out on the 15 mg powder samples at incremental rates of 10 °C/min from 25 to 1000 °C.

3. Results and Discussion

3.1. Chemical composition of CDW-based materials

Table 1 presents the chemical compositions of CDW-based materials obtained from seven different demolition sites. The main elements detected in the composition of HBs were oxygen, silicon, aluminum, iron and calcium. SiO_2 content of HBs varied between 42.1-57.7%, while Al_2O_3 was in the range of 13.7-16.2%. RCBs had SiO_2 and Al_2O_3 contents in the range of 45.8-59.9% and 13.5%-18.3%, respectively. The chemical composition of RTs was also found to be close to other clayey materials with SiO_2 and Al_2O_3 ranges between 46.2-55.3% and 12.6-

16.3%, respectively. The properties of bricks and tiles largely depend on the manufacturing method and properties of raw materials used in their production (Brick Industry Association, 2006). Raw materials of bricks and tiles are soils containing high amounts of clay together with some silt. Bricks and tiles generally contain 50-60% silica, 20-30% alumina, 2-5% lime, <7% iron oxide and <1% magnesia (Pumnia et al., 2003). In the selection of raw materials, the quality of clay-based soils is one of the most important parameters controlling the performance of tiles and bricks. Illite, kaolinite and a reduced amount of montmorillonite are usually used as clay minerals (Sverguzova et al., 2016). Based on the aforementioned statements, the small differences registered in the chemical compositions of the clayey CDWs can be due to the type of raw materials used in materials' production together with impurities that may have been contained throughout such products' service life.

Unlike clayey CDWs, clear differences can be seen in the chemical compositions of concrete wastes. This was expected since the original concretes are mostly with diverse strength classes and components and subjected to different service exposure conditions. For example, the aggregates, which constitute a significant portion of the collected concrete waste, are very likely to be obtained from diverse sources and origins (*e.g.*, siliceous, calcareous). Considering that limestone (calcareous) aggregates are with low contents of SiO_2 and high contents of CaO and loss on ignition (LoI) (Aquino et al., 2010), concrete wastes collected from K and L sites seem to be produced with calcerous aggregates. As for materials from X, Y, and Z sites, which contain SiO_2 in the range of 54.7-56.9%, the original aggregates are likely to be siliceous, such as quartz and albite (Medina et al., 2015; Bui et al., 2018). Regarding the concrete wastes from M and N sites with close SiO_2 and CaO contents, they are likely to be prepared with silico-calcareous aggregates. It needs to be stated that the compositions of concrete wastes are not only dependent on the possible types of aggregates, but also on the aggregate-to-cement ratio, type/chemical composition of PC, and physical/chemical changes that can take place during the service life of these materials (Sánchez-Cotte et al., 2020).

Considering the limited availability of glass in demolition sites compared to other CDWs, only a single type of glass obtained from the K site was characterized in the study. Another reason for the selection of glass from a single site was due to that comparable glass types were utilized in residential constructions in general, with no significant differences in the materials' chemical compositions according to the literature (Jani and Hogland, 2014; Olofinnade et al., 2017). The chemical composition of glass waste comprised SiO_2, CaO and Na_2O concentrations of 65.4%, 9.0%, and 12.0% respectively, together with other minor oxides. In

accordance with the literature, this composition was found to be rather similar to that of other glass wastes obtained from different urban transformation and demolition sites (Varshneya and Mauro, 2019). As inferred from Table 1, the amount of silica in glass waste is slightly higher than other CDWs, although the amount of alumina is remarkably lower than all CDWs.

Table 1 Chemical composition of CDW-based clayey materials.

Demolition site notation	Chemical composition (%)								
	SiO_2	Al_2O_3	Fe_2O_3	CaO	MgO	K_2O	Na_2O	SO_3	LoI*
K-HB	54.0	16.2	7.62	6.82	2.58	2.99	0.34	0.69	3.43
L-HB	52.5	14.2	12.1	4.53	5.10	1.76	0.80	1.38	0.59
M-HB	56.8	15.8	8.24	3.13	2.41	2.88	0.32	1.48	0.77
N-HB	42.1	13.8	11.8	6.42	6.45	1.55	1.45	1.46	1.43
X-HB	48.9	13.7	11.0	7.44	4.82	2.07	0.37	1.47	3.02
Y-HB	52.5	14.9	8.59	4.06	2.65	2.74	0.44	0.52	1.99
Z-HB	57.7	14.7	7.90	3.97	2.24	2.43	-	0.42	3.15
K-RCB	55.1	16.7	8.20	3.59	2.63	2.94	0.53	3.70	1.51
L-RCB	55.0	15.5	11.7	2.79	2.86	2.42	0.26	0.21	0.26
M-RCB	59.2	18.3	7.72	2.78	2.35	2.77	0.42	1.41	0.73
N-RCB	45.8	13.5	11.9	7.81	5.55	1.88	0.98	1.88	3.90
X-RCB	52.6	14.8	8.31	4.64	2.78	2.45	0.69	0.95	2.92
Y-RCB	57.6	14.4	8.28	4.70	2.53	2.14	0.77	1.93	1.45
Z-RCB	59.9	13.6	7.40	5.20	2.27	2.02	0.93	2.31	1.30
K-RT	47.7	13.7	14.0	7.62	6.54	1.18	0.69	0.72	0.69
L-RT	51.6	13.2	8.95	9.83	4.30	1.98	0.59	0.86	2.73
M-RT	53.4	16.3	9.49	5.27	3.64	2.78	0.39	1.61	1.67
N-RT	46.2	12.6	12.1	9.88	5.41	1.16	1.13	0.40	2.59
X-RT	50.8	14.4	10.5	7.09	4.55	2.28	0.46	0.83	2.13
Y-RT	55.3	14.8	8.28	6.69	4.72	2.11	1.04	1.16	1.45
Z-RT	54.7	13.2	9.28	6.90	4.01	1.92	0.68	0.54	2.20
K-C	4.34	1.24	0.76	49.7	0.81	0.17	0.02	-	37.7
L-C	4.16	1.34	0.87	50.2	0.82	0.16	0.02	-	38.7
M-C	37.4	10.7	3.82	21.2	1.29	2.22	1.96	0.54	19.7
N-C	34.8	4.36	3.45	27.2	4.46	0.79	0.19	1.32	22.0
X-C	56.9	8.76	4.01	11.8	1.50	1.53	1.16	0.85	9.76
Y-C	56.0	8.88	4.23	11.8	1.51	1.51	1.03	0.72	8.84
Z-C	54.7	9.76	4.22	11.5	1.52	1.53	2.02	0.80	8.94
K-G	65.4	0.98	0.54	8.97	3.73	0.14	12.0	0.65	1.60

*: Loss on ignition

3.2. Particle size distribution of CDW-based materials

Particle size distributions of CDW-based materials subjected to the same crushing and grinding processes are presented in Fig. 2. In addition, their related d(0.1), d(0.5), and d(0.9) particle sizes are presented in Table 2. The particle size distributions of most clayey materials were found to be similar, except for HB, RCB, and RT obtained from sites Y, X, and X, respectively, which presented some differences. This can be also seen from the particle diameter results shown in Table 2. For example, the d(0.5) values of HB from Y site and RCB

from X site were more than three times higher than those of other HBs and RCBs; whereas the d(0.9) value of RT from X site was almost three times higher than other RTs. These differences registered under the same crushing and grinding conditions can be due to various brittleness levels and impurities of each collected sample, since no clear relation was noticed with their respective chemical compositions. It can be stated that the grindability and its associated particle size distribution can be greatly affected by material characteristics such as strength and nature, brittleness, hardness, smoothness, stickiness and also moisture content (Meghwal and Goswami, 2013). Also, the grindability is highly influenced by the presence of different phases such as quartz in varied amounts and intensities (Asensio et al., 2016).

According to the particle size distributions of concrete wastes presented in Fig. 2, samples from K and L sites showed small dissimilarities than other concrete wastes. Although the d(0.1) values were similar for all concrete wastes, the samples from K and L sites presented higher d(0.5) and d(0.9) values, implying also coarser particle sizes (Table 2). By comparing these results with the chemical composition of concrete wastes, samples from K and L sites were shown to be produced with calcareous aggregates. Thus, the coarser particle size distribution of concrete wastes from K and L sites can be related to the possible agglomeration of limestone particles during pulverization, which reduced their grinding efficiency (Ghiasvand et al., 2015).

According to the particle size distribution results (Fig. 2), glass waste has coarser particle size distribution than most of other CDW-based materials. This can be confirmed from the d(0.5) value, which is more than two times higher than those of all CDWs, except for RCB obtained from X site. The amorphous nature of glass waste is likely to be one of the important reasons for its coarser particle size obtained under the same crushing/grinding procedures applied to other CDWs. In accordance with (Stekla, 2016), brittle and amorphous nature of glass causes it to have a sharp-edged grain morphology causing it to have a higher tendency of agglomeration during grinding. In conclusion, its grindability is poorer compared to other CDW-based materials, which are softer than glass (Ulugöl et al., 2021).

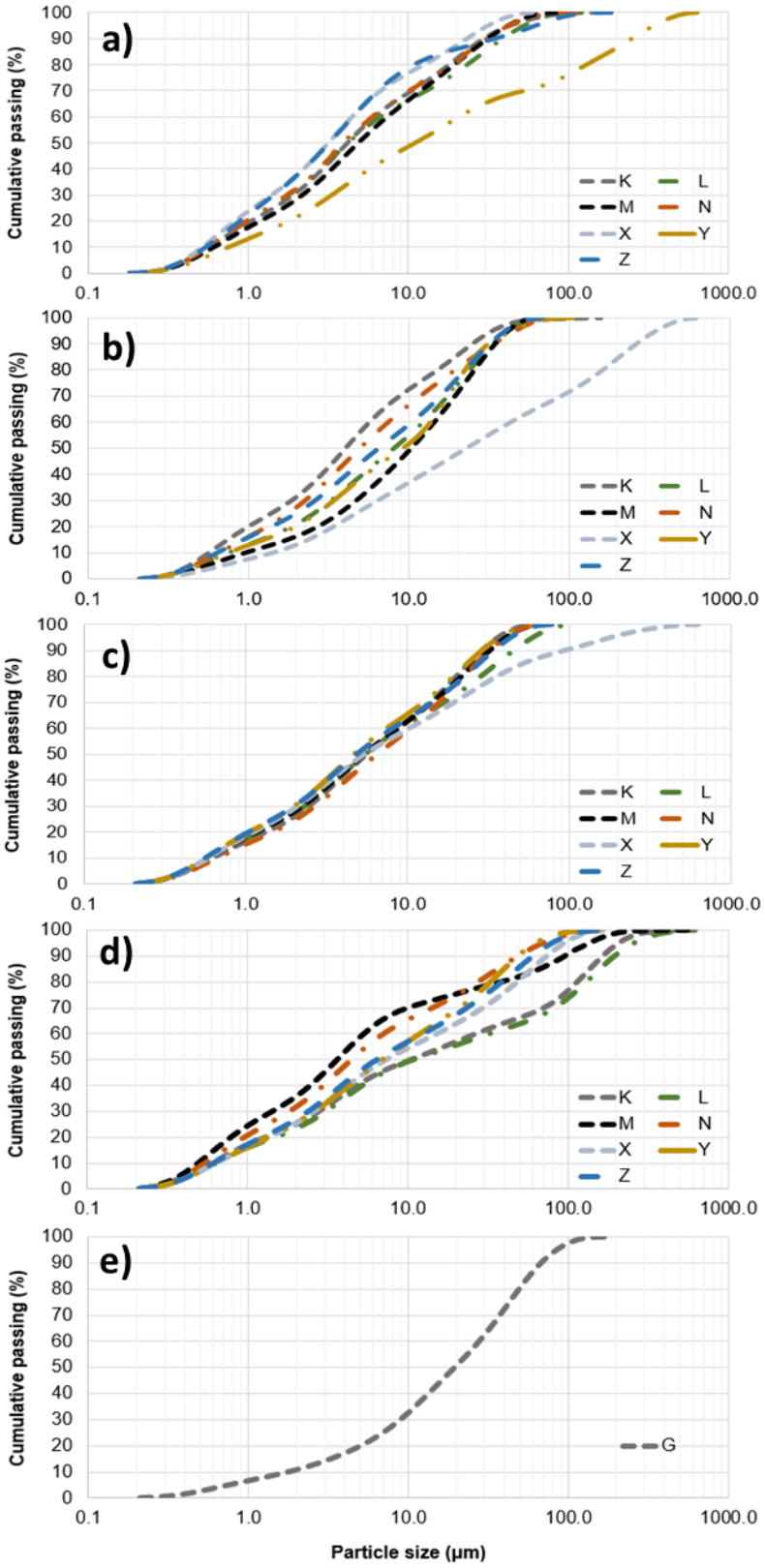

Fig. 2 Particle size distrubition of CDW-based clayey materials, a) HB; b) RCB; c) RT; d) C; e) G.

Table 2 Characteristic particle diameters of CDW-based materials (units are in μm).

Demolition site notation	d(0.1)	d(0.5)	d(0.9)	Demolition site notation	d(0.1)	d(0.5)	d(0.9)
K-HB	0.596	4.18	29.6	**K-RT**	0.621	5.55	28.6
L-HB	0.567	4.20	38.6	**L-RT**	0.603	5.50	45.4
M-HB	0.612	4.88	31.4	**M-RT**	0.592	5.41	32.1
N-HB	0.557	4.19	31.2	**N-RT**	0.663	6.49	32.3
X-HB	0.519	3.18	23.2	**X-RT**	0.587	5.40	93.4
Y-HB	0.754	10.1	247.4	**Y-RT**	0.566	4.64	28.5
Z-HB	0.543	3.21	34.6	**Z-RT**	0.559	4.85	34.0
K-RCB	0.566	4.03	24.9	**K-C**	0.597	10.4	163.5
L-RCB	0.742	8.02	33.2	**L-C**	0.620	10.8	193.4
M-RCB	0.951	10.3	34.6	**M-C**	0.486	3.60	95.0
N-RCB	0.651	4.97	34.2	**N-C**	0.536	4.43	48.6
X-RCB	1.403	22.7	260.2	**X-C**	0.626	7.29	73.3
Y-RCB	0.740	9.12	31.3	**Y-C**	0.635	6.91	48.4
Z-RCB	0.634	6.48	32.0	**Z-C**	0.610	6.36	60.1
				K-G	1.75	19.4	67.2

3.3. Crystalline nature of CDW-based materials

Structures observed as a result of XRD analyzes of CDW-based materials are presented in Fig. 3. Details of the observed peaks including the chemical formula and particle diffraction file (PDF) numbers, are also given in Table 3. According to XRD results, all clayey CDWs studied were with a semi-crystalline structure, with the main peaks being related to quartz and a broad hump centered between 2θ values of approximately 21° and 26°. Besides quartz, minor peaks related to other crystalline formations such as cristobalite, diopside, mullite, and akermanite, which consist of silica, alumina and calcium-based components were also observed. As was also shown in literature, quartz, which represents a substantial portion of the crystalline structure of clayey materials, is mostly unreactive and undergoes almost no change in intensity after interaction with the alkalies (Lee and Deventer, 2003). However, when these materials were calcined by heat treatment up to 800-1000 °C, their crystalline structure was disturbed, which results in the formation of amorphous alumina and silica and positively contributes to their pozzolanic activity (Tantawy, 2015; Cao et al., 2016). Although applying a further calcination treatment on the collected HB, RCB and RTs can ensure their use with greater mechanical performance, additional cost, energy, and time required for the calcination process may highly limit the outcomes of recycling applications.

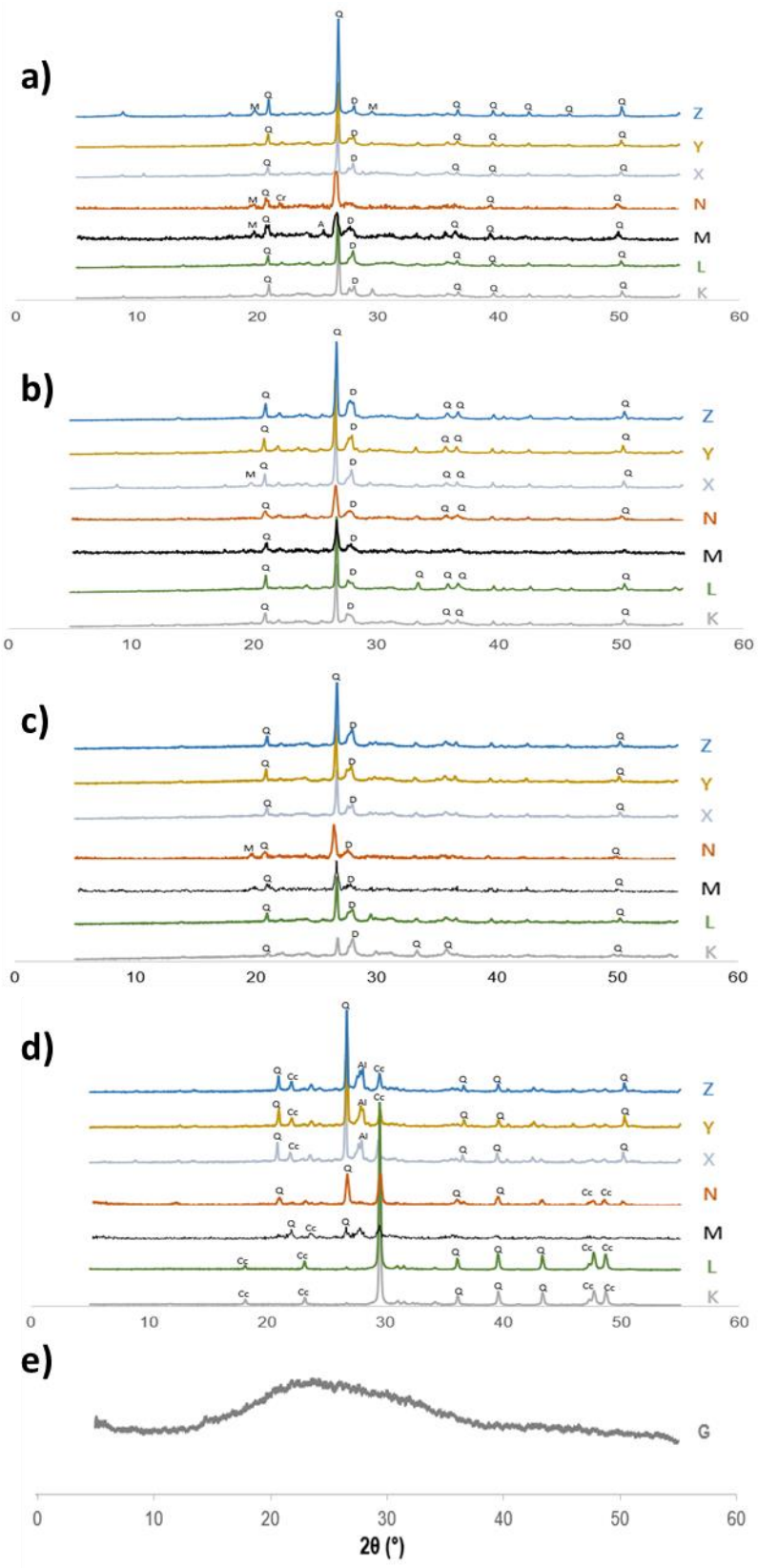

Fig. 3 XRD diffractograms of CDW-based materials, a) HB; b) RCB; c) RT; d) C; e) G

XRD diffractograms of different concrete wastes are given in Fig. 3 together with the chemical formula and PDF numbers of the identified peaks in Table 3. Fig. 3 shows that the

concrete wastes have also crystalline nature, with principal peaks of quartz, calcite and albite. However, significant differences were observed in the crystalline structures of concrete wastes compared to the clayey wastes with largely similar structures. Quartz peaks with higher intensity were observed in samples from X, Y, and Z sites, especially at around 2θ of 26°. While calcite was the dominant crystalline structure for the concrete wastes from K and L sites, a mixture of quartz and calcite was noticed at higher intensity in concrete wastes from M and N sites. It is notable that the intensities of different peaks are quite compatible with the chemical compositions of each sample. Another aspect to consider is that calcite peaks were found not only in concrete wastes produced with the calcareous aggregates but in all concrete wastes, which may be formed as a result of the carbonation of cement hydration products (Moreno-Pérez et al., 2018). According to the XRD diffractograms, the glass waste had a completely amorphous nature. As is known, the pozzolanic activity and alkaline activation efficiency of the materials are largely driven by their amorphousness (Ulugöl et al., 2021). However, the complete amorphousness of a material does not ensure that it will have excellent pozzolanic activity, because this property is also highly dependent on the chemical composition and fineness

Table 3 Types, PDF numbers, and chemical formulas of crystalline phases

Crystalline phase	Symbol	PDF number	Chemical formula
Quartz	Q	96-101-1160	SiO_2
Crystobalite	Cr	96-900-8230	SiO_2
Diopside	D	96-900-5280	$Al_{0.6}CaMg_{0.7}O_6Si_{1.7}$
Mullite	M	96-900-5502	Al_2O_5Si
Akermanite	A	96-900-6115	$AlCa_2Mg_{0.4}O_7Si_{1.5}$
Calcite	Cc	96-900-0968	$CaCO_3$
Albite	Al	96-154-0705	Ca_3O_5Si

3.4. Pozzolanic activity of CDW-based materials

3.4.1. Clayey materials

7-, 28-, and 90-day compressive strengths of the mortar samples were measured and their SAIs were calculated relative to the control samples (Fig. 4). All HB, RCB, and RTs had lower SAIs than the control samples with SAI of 100%, regardless of the curing age and demolition site from where they were collected. Comparing the results of different clayey materials, HB, RCB, and RT showed average SAI values of all ages of 84.5%, 86.3%, and 83.4%, respectively. In general, these differences are believed to be in relation with the previously shown variances

noted in the CDW material properties such as fineness, chemical composition and crystalline nature. Another reason for the differences noted in the pozzolanic activity of clayey CDWs can be the kiln temperature utilized in producing these materials, since lower firing temperatures have been reported to yield to lower pozzolanic activity (Pereira-de-Oliveira et al., 2012). As expected, the pozzolanic activity of clayey CDWs generally increased with the increased curing ages and contributed more to the compressive strength development at later ages (Zhao et al., 2020). This is related to the increased efficiency of materials with sufficient amounts of aluminosilicate oxides and fineness in binding $Ca(OH)_2$ in the presence of moisture over time to form C-S-H gels (O'Farrell et al., 2006; Pereira-de-Oliveira et al., 2012).

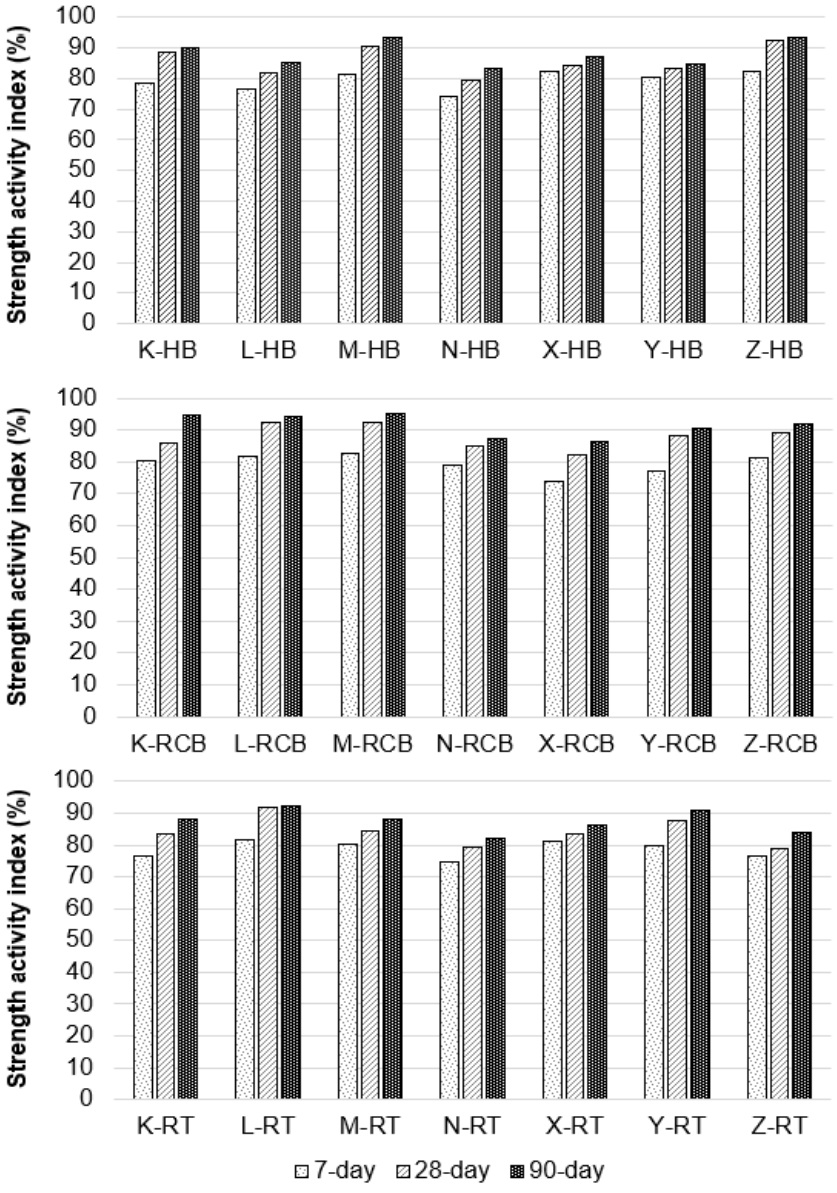

Fig. 4 Strength activity indexes of CDW-based clayey materials

According to the Fig. 4, among all HBs, although one of the weakest pozzolanic activity of HB from Y site (Y-HB) was in line with the material's coarser particle size distribution, X-HB with the finest particle size distribution did not exhibit the optimum pozzolanic activity. The highest SAI of M-HB at 90 days was both related to its highest SiO_2+Al_2O_3 content and fineness. It can generally be stated that for HBs, the applied crushing/grinding procedures were more efficient in reaching SAIs higher than 80% with the achievement of maximum d(0.5) and d(0.9) values of around 4 μm and 40 μm, respectively. Together with the high fineness of HB, SiO_2+Al_2O_3 content greater than 70% are the likely parameters to achieve an average SAI of at least 90% at 90 days.

Considering the pozzolanic activity of RCBs, it was observed that the M-RCB presented the greatest average SAIs with 82.7%, 92.6%, and 95.3% in 7, 28, and 90 days, respectively. This can be related to material's highest SiO_2+Al_2O_3 content (77.4%), finer particle size distribution and crystallinity level compared to most of other RCBs. Another point to stress is that, although the SiO_2+Al_2O_3 content of N-RCB was moderate, and L-RCB was with a relatively coarse particle size, SAIs of these materials were still higher than 87% after 90 days. This can be either due to suppression of the effect of relatively coarse particle size distribution (although below 45 μm) by adequate SiO_2+Al_2O_3 content thanks to better chemical interactions (Xiao et al., 2018), or suppression of relatively lower SiO_2+Al_2O_3 content by relatively finer particle size distribution thanks to the micro-filler effect besides pozzolanic activity (Cordeiro et al., 2008).

Considering the pozzolanic activity of RTs, it can be surprisingly seen that L-RT has the highest SAI values, especially at the early ages, although it is neither with the finest particle size distribution nor with the highest SiO_2+Al_2O_3 content. The supplementary cementitious materials can contribute to compressive strength not only thanks to pozzolanic activity but also with micro-aggregate effect, especially at the early ages (Zhao et al., 2020). Y-RT with the highest SiO_2+Al_2O_3 content (70.1%) showed the second-best pozzolanic activity after L-RT, and N-RT with the lowest SiO_2+Al_2O_3 content (58.8%) exhibited the worst pozzolanic activity at later ages. Unlike other RTs, mullite crystals observed in N-RT might also have caused poor reactivity.

3.4.2. Concrete waste

SAIs of concrete wastes were presented in Fig. 5. Similar to clayey CDWs, concrete wastes also showed lower SAIs than the control mixture. The average results of all ages for the diverse concrete wastes were 80.7%. The 90-day SAIs of concrete wastes were generally lower than

the 7- and 28-day values. This can be related to the fact that waste concrete contributes to the achievement of compressive strength at early ages thanks to unhydrated cementitious materials available in their surface leading to the formation of extra C-S-H gels (Horsakulthai, 2021). In a recent study, similar results were reached and it was concluded that waste concrete powder improved the hydration reaction by accelerating the formation of C-S-H gels due to its nucleus effect at early ages (*i.e.*, 7- and 28-day) (Huashan and Yujun, 2021). Based on these findings, it therefore seems that the amount of attached cement/mortar particles on the surface of concrete wastes highly control the contribution of these materials to the strength development of mortars incorporating them. Contrary to clayey CDWs, concrete wastes with high calcium and low silica contents were expected to be with poor pozzolanic activity (Kim and Choi, 2012). For example, according to (Antony and Nair, 2016), concrete waste powder was shown to exhibit substantially lower reactivity than roof tile powder in terms of lime reactivity test. In this study, concrete wastes were with lower average SAIs compared to clayey CDWs, especially at 90 days. However, some concrete wastes, such as M-C and Y-Cs, presented close or even better strength activity indexes than clayey CDWs at 7 and 28 days. Thus, the pozzolanic activity of this waste is closely related to its composition incorporating large shares of unhydrated cement grains, which likely contributes to the compressive strength development of the new mortars through further cement hydration rather than pozzolanic activity (Mas et al., 2012; Zhu et al., 2019; Juan-Valdes et al., 2021). This statement was approved by the mostly lower SAIs of concrete wastes at later curing age of 90 days. However, K-C and L-C with lower SiO_2+Al_2O_3 contents exhibited lower SAIs than other concrete wastes, implying for a possible contribution of this parameter to the strength development of C-based concretes. The important difference between the activity indexes of K-C and L-C, despite their similar chemical composition, particle size distribution and crystalline structures, also hints for the possible effects of impurities available on the surface of waste concrete particles.

3.4.3. Glass waste

According to the Fig. 5, G had lower SAIs compared to all other CDW-based materials. The values for 7, 28, and 90 days of curing were 71.8%, 76.5%, and 79.1%, respectively. Greater pozzolanic activity and reactivity were expected from the G due to its high silica content and amorphous nature. Furthermore, several investigations in the literature reported that G could exhibit very high pozzolanic activity at different ages (even at 90 days) (Shi et al., 2005; Afshinnia and Rangaraju, 2015). However, the G herein was with comparatively coarser particle size distribution compared to those in literature and other CDW-based materials, which

may be the main reason for the poor pozzolanic activity observed. This has been supported by a study in literature which stated that the level of fineness of G is the most fundamental parameter in determining its pozzolanic activity (Pereira-de-Oliveira et al., 2012). Here, it needs to be emphasized that G was not subjected to further grinding procedure for an easier comparison with other CDW-based materials, although it is highly likely to obtain better results at lower particle size of glass. The prepared powder presented a lower pozzolanic activity although it was with completely amorphous structure and this was mostly due to low Al_2O_3 content and relatively coarse particle size of the G.

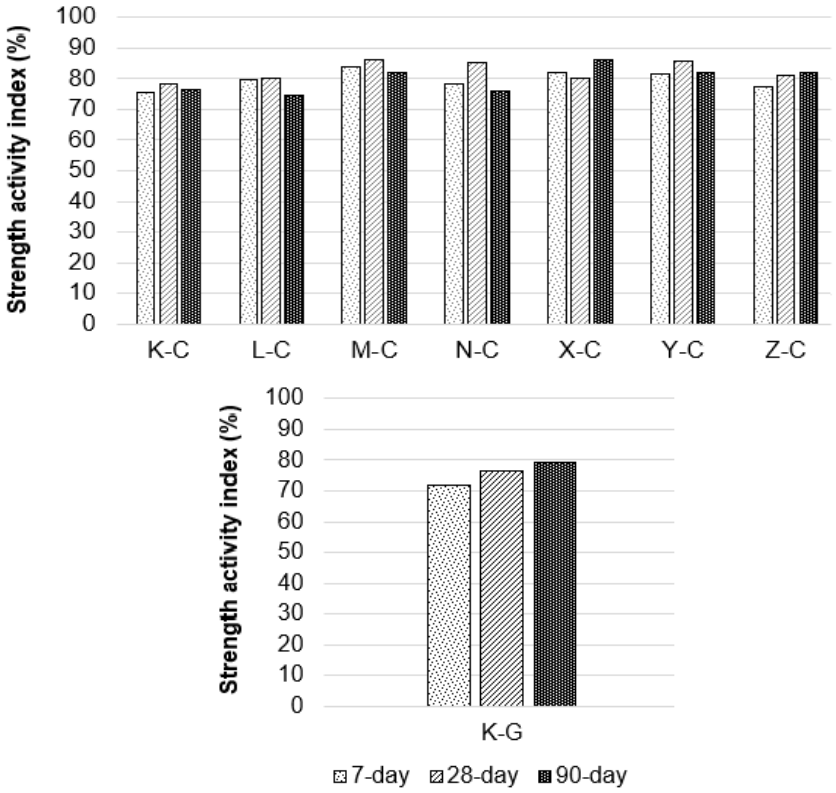

Fig. 5 Strength activity indexes of CDW-based concrete and glass.

3.5. Scanning electron microscopy and Energy-dispersive X-ray spectroscopy analysis

SEM micrographs and point EDX analysis results of mixtures produced with M-coded CDW-based materials and K-G were presented in Fig. 6 and Table 4, respectively. SEM micrographs of the specimens including M-coded CDW-based materials were found to be compact and homogeneous. While the reaction products of the specimens produced with clayey CDWs (*i.e.*, HB, RCB and RT) were generally well dispersed and showed a smooth surface, local crack formation in the specimen including C and partial agglomeration of the products in the specimen including G was observed. To interpret these circumstances and make it clear,

EDX analysis was performed at various points to reveal the presence of possible unreacted CDWs and their agglomeration and observe the reaction products whether formed as a result of cement hydration or pozzolanic reaction of CDW grains. The EDX analysis results showed that while the chemical compositions varied in several regions, the matrices generally had comparable atomic distributions. For instance, in the HB-included specimens, while similar chemical composition was observed at points 1,3 and 5, oxide values were lower and Ca values were higher at points 2 and 4. This indicates the presence of calcium-rich structures such as $Ca(OH)_2$ at points 2 and 4. Also, higher Al detection in the point 3 of the RCB-included mixture and in the point 1 of the RT-included mixture might be attributed to formation of C-A-S-H gel type. Also, significantly higher Si value at point 5 in the C-included mixture compared to other points might be attributed to the presence of unreacted C particles. In the EDX analysis of G-included mixture, all selected points from different locations exhibited identical chemical compositions.

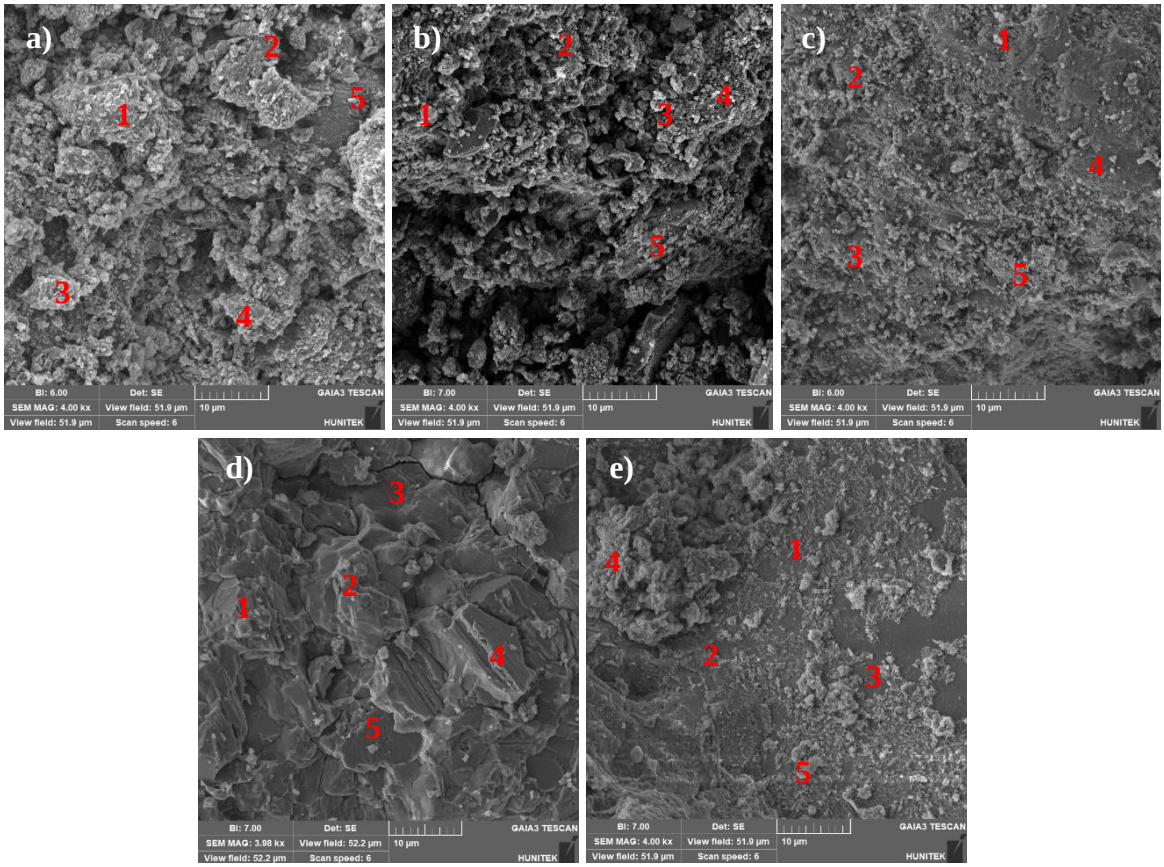

Fig. 6 SEM micrographs of the mixtures, a) M-HB; b) M-RCB; c) M-RT; d) M-C; e) K-G.

Table 4 EDX analysis results of the mixtures including M-coded CDW-based materials

CDW Component	Point No.	O	Ca	C	Si	Al	Fe
		(wt%)					
HB	1	53.8	29.8	16.3	0.10	0.00	0.10
	2	33.6	54.2	5.50	2.10	0.90	3.80
	3	48.2	29.9	11.3	6.80	2.20	1.70
	4	51.4	28.5	14.4	4.50	0.50	0.60
	5	25.9	63.4	4.20	4.20	0.70	1.60
RCB	1	44.6	25.6	15.3	9.30	3.10	2.00
	2	52.8	25.7	14.5	4.20	1.60	1.20
	3	59.6	8.90	13.2	10.0	7.00	1.30
	4	56.6	19.1	16.3	4.60	1.60	1.80
	5	55.2	22.9	13.4	7.00	0.80	0.70
RT	1	31.5	7.50	15.6	27.1	14.5	3.80
	2	54.5	29.6	14.6	0.90	0.40	0.10
	3	46.3	40.7	10.2	1.80	0.60	0.30
	4	50.8	31.4	16.0	1.60	0.20	0.00
	5	53.3	29.3	12.4	3.90	1.00	0.10
C	1	56.6	26.9	15.8	0.50	0.20	0.00
	2	45.1	43.3	11.5	0.00	0.00	0.00
	3	56.2	25.8	17.9	0.01	0.00	0.20
	4	57.6	20.5	17.9	3.00	0.50	0.40
	5	58.1	6.6	16.4	10.9	7.60	0.50
G	1	56.9	5.30	8.70	28.2	0.60	0.30
	2	52.6	7.80	11.4	27.2	0.70	0.30
	3	53.2	8.20	10.7	27.3	0.70	0.00
	4	47.3	11.7	11.5	28.4	0.80	0.60
	5	57.1	6.00	10.2	25.8	0.70	0.20

3.6. Thermogravimetry (TG/DTG) analysis

Thermogravimetry (TG/DTG) analysis of the mixtures included M-coded HB, RCB, RT, C and K-coded G and OPC paste were presented in Fig. 7. According to the TG/DTG analysis results, four different temperature regions were detected where remarkable differences appeared in weight change. In the first region where the temperature range is between approximately 30-110 °C, similar weight losses were encountered for all mixtures. The weight losses observed in this range can be attributed to the loss of evaporable water in the system (Alarcon-Ruiz et al., 2005). In the second region where the temperature range is between approximately 180-300 °C, it was observed that the M-RCB coded mixture experienced the highest weight loss, followed by M-RT, M-HB, K-G, M-C and OPC paste, respectively. As it is known from the literature, considering that the weight loss in the 180-300 °C range is generally caused by the loss of bound water from the decomposition of the C-S-H and loss of carboaluminate hydrates (Alarcon-Ruiz et al., 2005; Thongsanitgarn et al., 2014), it can be

concluded that, in the M-RCB coded mixture, the gel structure formation that will cause water loss is slightly higher than the other mixtures at the end of the 90-day curing. The significant pozzolanic activity of CDW-based materials contributed to the formation of extra C-S-H in the matrix in the long term. Next, the weight loss of OPC paste increased sharply in the temperature range arround 450–550 °C, while it was found that other mixtures incorporating CDW-based material exhibited significantly lower weight losses. The weight loss observed in this temperature range, where indicates the dehydroxylation of the calcium hydroxyde in general (Lorca et al., 2014), showed that CDW-based materials pozolanically combined with calcium hydroxyde which is the secondary hydration product of Portland cement and caused the decreasing amount of it. Finally, significant weight losses were also observed in the temperature range of 700-900 °C. The most severe weight loss of OPC paste in this temperature range, which is associated with the decarbonation of calcium carbonates formed as a result of carbonation of calcium hydroxide (Huang et al., 2019), indicates that it contains a higher proportion of calcium hydroxide than other mixtures containing CDW-based materials. This can be explained by the consumption of calcium hydroxide in mixtures containing CDW-based materials as a result of pozolanic reactions.

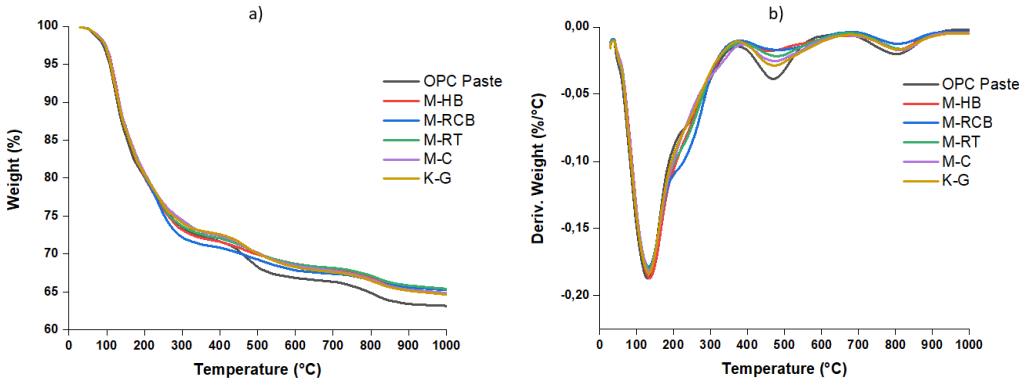

Fig. 7 TG/DTG analyses of the mixtures, a) TGA b) DTG.

4. Pearson correlation analysis

In order to statistically examine the influences of chemical composition (*i.e.*, SiO_2, Al_2O_3 and CaO) and fineness degrees (*i.e.*, d[0.1], d[0.5] and d[0.9]) of CDWs on the 7-, 28- and 90-day SAI values, Pearson's Correlation Coefficient analysis was performed. The results shown in Table 5 demonstrated that there is a strong positive relationship between the SiO_2 and Al_2O_3 concentration and the SAI values. In particular, when the relationship of SiO_2 and Al_2O_3 content with the 90-day SAI values is examined, it was seen that the Pearson correlation coefficient has a very high positive correlation with values of 0.65 and 0.835, respectively. On

458 the other hand, CaO had a negative relationship with the SAI values of CDW-substituted
459 mixtures. Also, the fineness degrees of the CDW-based materials (*i.e.*, d[0.1], d[0.5], d[0.9])
460 showed a negative correlation with SAI values at all ages, as discussed above. Another
461 interesting finding is that while the influence of d(0.1) and d(0.5) reduced with age, the
462 influence of d(0.9) increased with age. When comparing the results in Table 5, it can be seen
463 that fineness had a significant impact on SAI values at early ages (*i.e.*, 7- and 28-day), but the
464 influence of chemical composition became more prominent in 90-day SAI values.

465 **Table 5** Pearson correlation analysis of the selected parameters

		SiO_2	Al_2O_3	CaO	d(0.1)	d(0.5)	d(0.9)
7-day SAI	**Pearson corr.**	0.117	0.332	-0.1	-0.499**	-0.484**	-0.16
	Sig. (2-tailed)	0.547	0.078	0.607	0.008	0.008	0.406
	N	29	29	29	29	29	29
28-day SAI	**Pearson corr.**	0.35	0.567**	-0.375*	-0.23	-0.309	-0.342
	Sig. (2-tailed)	0.063	0.001	0.045	0.229	0.103	0.07
	N	29	29	29	29	29	29
90-day SAI	**Pearson corr.**	0.65**	0.835**	-0.731**	-0.094	-0.246	-0.439*
	Sig. (2-tailed)	0	0	0	0.627	0.198	0.017
	N	29	29	29	29	29	29

466 * : Correlation is significant at the 0.01 level (2-tailed)
467 **: Correlation is significant at the 0.05 level (2-tailed)

468 **5. Conclusions**

469 A detailed characterization of CDW-based hollow brick, red clay brick, roof tile, concrete,
470 and glass obtained from various demolition sites was performed in this study.
471 Physical/chemical properties and crystalline structures of these materials were determined and
472 possible interrelationships of these properties and the pozzolanic activity of each material were
473 evaluated. The following conclusions can be made:

474 • Chemical compositions of HB, RCB, and RTs were found almost in the same range,
475 except for some differences related to their original raw materials/production method.
476 Larger differences were reported in the chemical compositions of Cs, which highly
477 depend on the type/content of cement and aggregates used in the original concretes. G
478 sample was with slightly higher silica content and lower alumina than all CDWs.
479 • Most of HB, RCB, RT, and Cs have reached to similar particle size distributions under
480 the same crushing/grinding procedures, although some materials presented coarser
481 particles because of the presence of the impurities and inherent hardness. Compared to
482 other CDWs, G showed coarser particle size distribution after same crushing/grinding.

- XRD analyses revealed a semi-crystalline structure for all HB, RCB, and RTs while a crystalline structure for all Cs, however, with clear differences in the quartz and calcite peaks between clayey materials and Cs. G presented a clear amorphous structure unlike other CDWs.
- Average SAIs of all ages were 84.5%, 86.3%, 83.4%, 80.7%, and 75.8% for HB, RCB, RT, C, and G, respectively. Clayey CDWs contributed to mechanical strength through their sufficient fineness and aluminosilicate oxide contents. Also, clayey CDWs can be utilized together without any selection/separation process since their SAIs are quite comparable to each other with only slight differences. However, the contribution of Cs was more related to the possible effects of hydration of the unreacted cementitious particles. On the other hand, G was found to have the weakest pozzolanic activity due to its coarser grain size distribution compared to other CDWs.
- The SAIs of all CDWs, irrespective of the origin and type of CDWs, were found acceptable for their use as SCMs in the PC-based systems, since their minimum average SAI was higher than 75% specified in ASTM C618.
- It was micromechanically confirmed by SEM/EDX and TGA/DTG analysis that CDW-based materials are pozolanically combined with calcium hydroxide and contribute to the formation of extra C-S-H gel by consuming calcium hydroxide.

Although one of the important criteria controlling the pozzolanic activity is the level of fineness reached for each CDW, materials' SiO_2+Al_2O_3 contents seem to highly influence the results. Particularly, when CDWs with similar finenesses were compared, materials with higher SiO_2+Al_2O_3 contents displayed better pozzolanic activity. It was suggested that the SAI of G sample can be improved by achieving higher fineness for this material. In this study, no further grinding was applied to materials since it would be more economical and ecological to prepare all CDW-based materials together in an optimum way without sorting and separation procedures. However, this seems inappropriate, especially when the nature of CDWs is different. Thus, it is recommended to separately test each collected material from various sites. It is also important to reach the adequate fineness for each material for an optimized performance of the newly developed materials.

Declaration of competing interest

The author declares that they have no known competing financial interests or personal relationships that could have appeared to influence the work reported in this paper.

Funding

This project has received funding from the European Union's Horizon 2020 research and innovation programme under the Marie Skłodowska-Curie grant agreement No 894100 and European Union's Horizon 2020 Research and Innovation Programme's financial assistance under Grant Agreement No: 869336 and Acronym: ICEBERG.

Acknowledgments

The authors gratefully acknowledge the Newton Prize 2020. This publication is a part of doctoral dissertation work by the first author in the Academic Program of Civil Engineering, Institute of Science, Hacettepe University.

References

Afshinnia K, Rangaraju PR (2015) Influence of fineness of ground recycled glass on mitigation of alkali–silica reaction in mortars. Construct. Build. Mater. 81, 257-267. https://doi.org/10.1016/j.conbuildmat.2015.02.041

Ajayi SO, Oyedele LO, Akinade OO, Bilal M, Owolabi HA, Alaka HA and Kadiri KO (2016) Reducing waste to landfill: A need for cultural change in the UK construction industry. J. Build. Eng. 5, 185-193. https://doi.org/10.1016/j.jobe.2015.12.007

Alarcon-Ruiz L, Platret G, Massieu E, Ehrlacher A (2005) The use of thermal analysis in assessing the effect of temperature on a cement paste. Cement Concrete Res. 35(3), 609-613. https://doi.org/10.1016/j.cemconres.2004.06.015

Antony J and Nair DG (2016) Potential of construction and demolished wastes as pozzolana. Procedia Technol. 25, 194-200. https://doi.org/10.1016/j.protcy.2016.08.097

Aquino C, Inoue M, Miura H, Mizuta M and Okamoto T (2010) The effects of limestone aggregate on concrete properties. Construct. Build. Mater. 24(12), 2363-2368. https://doi.org/10.1016/j.conbuildmat.2010.05.008

538 Asensio E, Medina C, Frías M and de Rojas MIS (2016) Characterization of ceramic-based
539 construction and demolition waste: use as pozzolan in cements. J. Am. Ceram. Soc. 99(12),
540 4121-4127. https://doi.org/10.1111/jace.14437

541 ASTM C39/C39M-21 (2021) Standard test method for compressive strength of cylindrical
542 concrete specimens. *ASTM International, West Conshohocken, PA.*
543 https://doi.org/10.1520/C0039_C0039M-21

544 ASTM C618-19 (2019) Standard specification for coal fly ash and raw or calcined natural
545 pozzolan for use in concrete. *ASTM International, West Conshohocken, PA.*
546 https://doi.org/10.1520/C0039_C0039M-21

547 Bakhtyar B, Kacemi T and Nawaz MA (2017) A review on carbon emissions in Malaysian
548 cement industry. Int. J. Energy Econ. Policy 7(3), 282-286.

549 Brick Industry Association (2006) Manufacturing of Brick, Tech. Notes on Brick Construct.
550 https://www.gobrick.com/docs/default-source/read-research-documents/technicalnotes/9-
551 manufacturing-of-brick.pdf?sfvrsn=0

552 Bui NK, Satomi T and Takahashi H (2018) Enhancement of recycled aggregate concrete
553 properties by a new treatment method. Int. J. Geomate 14(41), 68-76.
554 https://doi.org/10.21660/2018.41.11484

555 Cao Z, Cao Y, Dong H, Zhang J and Sun C (2016) Effect of calcination condition on the
556 microstructure and pozzolanic activity of calcined coal gangue. Int. J. Miner. Process. 146, 23-
557 28. https://doi.org/10.1016/j.minpro.2015.11.008

558 Chan CC, Thorpe D and Islam M (2015) An evaluation carbon footprint in fly ash based
559 geopolymer cement and ordinary Portland cement manufacture. *International Conference on*
560 *Industrial Engineering and Engineering Management* (pp. 254-259).
561 https://doi.org/10.1109/IEEM.2015.7385647

562 Cheng H (2016) Reuse research progress on waste clay brick. Procedia Environ. Sci. 31, 218-
563 226. https://doi.org/10.1016/j.proenv.2016.02.029

564 Cordeiro GC, Toledo Filho RD, Tavares LM and Fairbairn EMR (2008) Pozzolanic activity
565 and filler effect of sugar cane bagasse ash in Portland cement and lime mortars. Cem. Concr.
566 Compos. 30(5), 410-418. https://doi.org/10.1016/j.cemconcomp.2008.01.001

Eurostat (2015) Eurostat statistics explained, Waste statistics. http://ec.europa.eu/eurostat/statistics-explained/index.php/Waste_statistics.

Ghiasvand E, Ramezanianpour AA and Ramezanianpour AM (2015) Influence of grinding method and particle size distribution on the properties of Portland-limestone cements. Mater. Struct. 48(5), 1273-1283. https://doi.org/10.1617/s11527-013-0232-0

Horsakulthai V (2021) Effect of recycled concrete powder on strength, electrical resistivity, and water absorption of self-compacting mortars. Case Studies in Construct. Mater. 15, e00725. https://doi.org/10.1016/j.cscm.2021.e00725

Huang G, Pudasainee D, Gupta R, Liu, WV (2019) Hydration reaction and strength development of calcium sulfoaluminate cement-based mortar cured at cold temperatures. Construct. Build. Mater. 224, 493-503. https://doi.org/10.1016/j.conbuildmat.2019.07.085

Huashan YANG and Yujun CHE (2021) Influences of Waste Concrete Powder on the Strength Development and Hydration Products of Mortar Containing Fly Ash. Mater. Sci. https://doi.org/10.5755/j02.ms.25591

Ilcan H, Sahin O, Kul A, Ozcelikci E, Sahmaran M (2023) Rheological property and extrudability performance assessment of construction and demolition waste-based geopolymer mortars with varied testing protocols. Cem. Concr. Compos. 136, 104891. https://doi.org/10.1016/j.cemconcomp.2022.104891

Jain P, Powell, J and Tolaymat T (2015) Methodology to estimate the quantity, composition, and management of construction and demolition, debris in the United States. US Environ. Prot. Agency EPA/600/R-15/111

Jani Y and Hogland W (2014) Waste glass in the production of cement and concrete–A review. J. Environ. Chem. Eng. 2(3), 1767-1775. https://doi.org/10.1016/j.jece.2014.03.016

Juan-Valdes A, Rodriguez-Robles D, Garcia-Gonzalez J, de Rojas Gómez MIS, Guerra-Romero MI, De Belie N and Morán-del Pozo JM (2021) Mechanical and microstructural properties of recycled concretes mixed with ceramic recycled cement and secondary recycled aggregates. A viable option for future concrete. Construct. Build. Mater. https://doi.org/10.1016/j.conbuildmat.2020.121455

595 Kim YJ and Choi YW (2012) Utilization of waste concrete powder as a substitution material
596 for cement. Construct. Build. Mater. 30, 500-504.
597 https://doi.org/10.1016/j.conbuildmat.2011.11.042

598 Komnitsas K, Zaharaki D, Vlachou A, Bartzas G and Galetakis M (2015) Effect of synthesis
599 parameters on the quality of construction and demolition wastes (CDW) geopolymers. Powder
600 Technol. 26(2), 368-376. https://doi.org/10.1016/j.apt.2014.11.012

601 Lee WKW and Van Deventer JSJ (2003) Use of infrared spectroscopy to study
602 geopolymerization of heterogeneous amorphous aluminosilicates. *Langmuir* 19(21), 8726-
603 8734. https://doi.org/10.1021/la026127e

604 Li LG, Lin ZH, Chen GM, Kwan AKH and Li ZH (2019) Reutilization of clay brick waste in
605 mortar: Paste replacement versus cement replacement. J. Mater. Civ. Eng. 31(7), 04019129.
606 https://doi.org/10.1061/(ASCE)MT.1943-5533.0002794

607 Lorca P, Calabuig R, Benlloch J, Soriano L, Payá J (2014) Microconcrete with partial
608 replacement of Portland cement by fly ash and hydrated lime addition. Mater. Des. 64, 535-
609 541. https://doi.org/10.1016/j.matdes.2014.08.022

610 Mahmoodi O, Siad H, Lachemi M, Dadsetan S and Sahmaran M (2020) Optimization of brick
611 waste-based geopolymer binders at ambient temperature and pre-targeted chemical parameters.
612 J. Clean. Prod. 268, 122285. https://doi.org/10.1016/j.jclepro.2020.122285

613 Mas B, Cladera A, Bestard J, Muntaner D, López CE, Piña S and Prades J (2012) Concrete
614 with mixed recycled aggregates: Influence of the type of cement. Construct. Build. Mater. 34,
615 430-441. https://doi.org/10.1016/j.conbuildmat.2012.02.092

616 Medina C, Zhu W, Howind T, Frías M and De Rojas MS (2015) Effect of the constituents
617 (asphalt, clay materials, floating particles and fines) of construction and demolition waste on
618 the properties of recycled concretes. Construct. Build. Mater. 79, 22-33.
619 https://doi.org/10.1016/j.conbuildmat.2014.12.070

620 Meghwal M and Goswami TK (2013) Evaluation of size reduction and power requirement in
621 ambient and cryogenically ground fenugreek powder. Adv. Powder Technol. 24(1), 427-435.
622 https://doi.org/10.1016/j.apt.2012.09.005

623 Menegaki M and Damigos D (2018) A review on current situation and challenges of
624 construction and demolition waste management. Curr. Opin. Green Sust. Chem. 13, 8-15.
625 https://doi.org/10.1016/j.cogsc.2018.02.010

626 Mir N, Khan SA, Kul A, Sahin O, Ozcelikci E, Sahmaran M, Koc M (2023) Construction and
627 demolition waste-based self-healing geopolymer composites for the built environment: An
628 environmental profile assessment and optimization. Construct. Build. Mater. 369, 130520.
629 https://doi.org/10.1016/j.conbuildmat.2023.130520

630 Monteiro PJ, Miller SA and Horvath A (2017) Towards sustainable concrete. Nat. Mater. 16(7),
631 698-699.

632 Moreno-Pérez E, Hernández-Ávila J, Rangel-Martínez Y, Cerecedo-Sáenz E, Arenas-Flores
633 A, Reyes-Valderrama M and Salinas-Rodríguez E (2018) Chemical and mineralogical
634 characterization of recycled aggregates from construction and demolition waste from Mexico
635 city. Miner. 8(6), 237. https://doi.org/10.3390/min8060237

636 Mucsi G, Halyag Papné N, Ulsen C, Figueiredo PO and Kristály F (2021) Mechanical
637 Activation of Construction and Demolition Waste in Order to Improve Its Pozzolanic
638 Reactivity. ACS Sust. Chem. Eng. 9(9), 3416-3427.
639 https://doi.org/10.1021/acssuschemeng.0c05838

640 Naceri A and Hamina MC (2009) Use of waste brick as a partial replacement of cement in
641 mortar. Waste Manag. 29(8), 2378-2384. https://doi.org/10.1016/j.wasman.2009.03.026

642 O'Farrell M, Sabir BB and Wild S (2006) Strength and chemical resistance of mortars
643 containing brick manufacturing clays subjected to different treatments. Cem. Concr. Compos.
644 28(9), 790-799. https://doi.org/10.1016/j.cemconcomp.2006.05.014

645 Oliveira TC, Dezen BG and Possan E (2020) Use of concrete fine fraction waste as a
646 replacement of Portland cement. J. Clean. Prod. 273, 123126.
647 https://doi.org/10.1016/j.jclepro.2020.123126

648 Olofinnade OM, Ede AN and Ndambuki JM (2017) Experimental investigation on the effect
649 of elevated temperature on compressive strength of concrete containing waste glass powder.
650 Int. J. Eng. Technol. Innov. 7(4), 280-291.

651 Ozcelikci E, Kul A, Gunal MF, Ozel BF, Yildirim G, Ashour A, Sahmaran M (2023a) A
652 comprehensive study on the compressive strength, durability-related parameters and

653 microstructure of geopolymer mortars based on mixed construction and demolition waste. J.
654 Clean. Prod. 396, 136522. https://doi.org/10.1016/j.jclepro.2023.136522

655 Ozcelikci E, Sahmaran M (2023b) Characterization and value-added application of low-quality
656 concrete waste based recycled aggregates. Mater. Today Proc.
657 https://doi.org/10.1016/j.matpr.2023.05.217

658 Pereira-de-Oliveira LA, Castro-Gomes JP and Santos PM (2012) The potential pozzolanic
659 activity of glass and red-clay ceramic waste as cement mortars components. Construct. Build.
660 Mater. 31, 197-203. https://doi.org/10.1016/j.conbuildmat.2011.12.110

661 Praneeth S, Guo R, Wang T, Dubey BK and Sarmah AK (2020) Accelerated carbonation of
662 biochar reinforced cement-fly ash composites: enhancing and sequestering CO2 in building
663 materials. Construct. Build. Mater. 244, 118363.
664 https://doi.org/10.1016/j.conbuildmat.2020.118363

665 Punmia BC, Jain AK and Jain AK (2003) Basic civil engineering. *Firewall Media.*

666 Rashad AM and Zeedan SR (2011) The effect of activator concentration on the residual
667 strength of alkali-activated fly ash pastes subjected to thermal load. Construct. Build. Mater.
668 25(7), 3098-3107. https://doi.org/10.1016/j.conbuildmat.2010.12.044

669 Robayo-Salazar RA, Rivera JF and de Gutiérrez RM (2017) Alkali-activated building materials
670 made with recycled construction and demolition wastes. Construct. Build. Mater. 149, 130-
671 138. https://doi.org/10.1016/j.conbuildmat.2017.05.122

672 Roussat N, Méhu J, Abdelghafour M and Brula P (2008) Leaching behaviour of hazardous
673 demolition waste. Waste Manag. 28(11), 2032-2040.
674 https://doi.org/10.1016/j.wasman.2007.10.019

675 Sánchez-Cotte EH, Pacheco-Bustos CA, Fonseca A, Triana YP, Mercado R, Yepes-Martínez
676 J and Lagares Espinoza RG (2020) The chemical-mineralogical characterization of recycled
677 concrete aggregates from different sources and their potential reactions in asphalt mixtures.
678 Mater. 13(24), 5592. https://doi:10.3390/ma13245592

679 Scrivener KL and Kirkpatrick RJ (2008) Innovation in use and research on cementitious
680 material. Cement Concrete Res. 38(2), 128-136.
681 https://doi.org/10.1016/j.cemconres.2007.09.025

682 Shi C, Wu Y, Riefler C and Wang H (2005) Characteristics and pozzolanic reactivity of glass
683 powders. Cement Concrete Res. 35(5), 987-993.
684 https://doi.org/10.1016/j.cemconres.2004.05.015

685 Stafford FN, Dias AC, Arroja L, Labrincha JA and Hotza D (2016) Life cycle assessment of
686 the production of Portland cement: a Southern Europe case study. J. Clean. Prod. 126, 159-
687 165. https://doi.org/10.1016/j.jclepro.2016.02.110

688 STEKLA OSDR (2016) Evaluation of the grindability of recycled glass in the production of
689 blended cements. *EVALUATION* 729, 734. https://doi.org/10.17222/mit.2015.184

690 Sverguzova SV, Sapronova ZA, Starostina IV (2016) Disposal of synthetic surfactants-
691 containing wastewater treatment sludge in the ceramic brick production. Procedia Eng. 150,
692 1610-1616. https://doi: 10.1016/j.proeng.2016.07.138

693 Tantawy MA (2015) Characterization and pozzolanic properties of calcined alum sludge.
694 Mater. Res. Bull. 61, 415-421. https://doi.org/10.1016/j.materresbull.2014.10.042

695 Thongsanitgarn P, Wongkeo W, Chaipanich A, Poon CS (2014) Heat of hydration of Portland
696 high-calcium fly ash cement incorporating limestone powder: Effect of limestone particle size.
697 Construct. Build. Mater. 66, 410-417. https://doi.org/10.1016/j.conbuildmat.2014.05.060

698 Turner LK and Collins FG (2013) Carbon dioxide equivalent (CO2-e) emissions: A
699 comparison between geopolymer and OPC cement concrete. Construct. Build. Mater. 43, 125-
700 130. https://doi.org/10.1016/j.conbuildmat.2013.01.023

701 Ulugöl H, Kul A, Yıldırım G, Şahmaran M, Aldemir A, Figueira D and Ashour, A (2021)
702 Mechanical and microstructural characterization of geopolymers from assorted construction
703 and demolition waste-based masonry and glass. J. Clean. Prod. 280, 124358.
704 https://doi.org/10.1016/j.jclepro.2020.124358

705 Varshneya AK and Mauro JC (2019) Fundamentals of inorganic glasses. *Elsevier*

706 Wu H, Zuo J, Zillante G, Wang J and Yuan H (2019) Construction and demolition waste
707 research: a bibliometric analysis. Archit. Sci. Rev. 62(4), 354-365.
708 https://doi.org/10.1080/00038628.2018.1564646

709 Xiao J, Ma Z, Sui T, Akbarnezhad A and Duan Z (2018) Mechanical properties of concrete
710 mixed with recycled powder produced from construction and demolition waste. J. Clean. Prod.
711 188, 720-731. https://doi.org/10.1016/j.jclepro.2018.03.277

712 Yıldırım G, Kul A, Özçelikci E, Şahmaran M, Aldemir A, Figueira D and Ashour A (2021)
713 Development of alkali-activated binders from recycled mixed masonry-originated waste. J.
714 Build. Eng. 33, 101690. https://doi.org/10.1016/j.jobe.2020.101690

715 Yildirim G, Ashour A, Ozcelikci E, Gunal MF, Ozel BF (2022) Development of Geopolymer
716 Binders with Mixed Construction and Demolition Waste-Based Materials. Eng. Proc. 17(1), 4.
717 https://doi.org/10.3390/engproc2022017004

718 Zhang C, Hu M, Di Maio F, Sprecher B, Yang X, Tukker A. (2022). An overview of the waste
719 hierarchy framework for analyzing the circularity in construction and demolition waste
720 management in Europe. Sci. Total Environ. 803, 149892.
721 https://doi.org/10.1016/j.scitotenv.2021.149892

722 Zhang Z, Provis JL, Reid A and Wang H (2014) Geopolymer foam concrete: An emerging
723 material for sustainable construction. Construct. Build. Mater. 56, 113-127.
724 https://doi.org/10.1016/j.conbuildmat.2014.01.081

725 Zhao Y, Gao J, Liu C, Chen X and Xu Z (2020) The particle-size effect of waste clay brick
726 powder on its pozzolanic activity and properties of blended cement. J. Clean. Prod. 242,
727 118521. https://doi.org/10.1016/j.jclepro.2019.118521

728 Zheng L, Wu H, Zhang H, Duan H, Wang J, Jiang W, Dong B, Liu G and Song Q (2017)
729 Characterizing the generation and flows of construction and demolition waste in China.
730 Construct. Build. Mater. 136, 405-413. https://doi.org/10.1016/j.conbuildmat.2017.01.055

731 Zhu P, Mao X and Qu W (2019) Investigation of recycled powder as supplementary
732 cementitious material. Mag. Concr. Res. 71(24), 1312-1324.
733 https://doi.org/10.1680/jmacr.18.00513